



Interfacial Stress Transfer and Property Mismatch in Discontinuous Nanofiber/Nanotube Composite Materials

L. Roy Xu* and Sreeparna Sengupta

*Department of Civil and Environmental Engineering & Interdisciplinary Materials Science Program,
VU Station B 351831, 2301 Vanderbilt Place, Vanderbilt University, Nashville, Tennessee 37235, USA*

Novel nanotubes/nanofibers with high strength and stiffness did not lead to high failure strengths/strains of nanocomposite materials. Therefore, the interfacial stress transfer and possible stress singularities, arising at the interfacial ends of discontinuous nanofibers embedded in a matrix, subjected to tensile and shear loading, were investigated by finite element analysis. The effects of Young's moduli and volume fractions on interfacial stress distributions were studied. Round-ended nanofibers were proposed to remove the interfacial singular stresses, which were caused by highly stiffness mismatch of the nanoscale reinforcement and the matrix. However, the normal stress induced in the nanofiber through interfacial stress transfer was still less than 2 times that in the matrix. This stress value is far below the high strength of the nanofiber. Therefore, the load transfer efficiency of discontinuous nanofibers or nanotube composites is very low. Hence, nanofibers or nanotubes in continuous forms, which also preclude the formation of singular interfacial stress zones, are recommended over discontinuous nanofibers to achieve high strengths in nanocomposite materials.

Keywords: Nanocomposites, Interfacial Stress, Property Mismatch, Stress Singularity, Finite Element Analysis.

1. INTRODUCTION

Since carbon nanotubes have extraordinary mechanical properties, they tend to be used as reinforcements in polymers and other matrices to form so-called "nanocomposite materials."^{1–10} Nanocomposites are a novel class of composite materials where one of the constituents has dimensions in the range 1–100 nm. Wagner et al.⁵ reported that load transfer through a shear stress mechanism was seen at the molecular level. It has been reported that nanotubes increase composite strength by as much as 25%.^{6,7} Alternative reinforcement materials for nanocomposites include nanofibers, nanoplatelets, nanoclays, etc. These reinforcements are functionalized with additives, thereby resulting in a strong interfacial bond with the matrix. Generally, the three main mechanisms of interfacial load transfer are micromechanical interlocking, chemical bonding, and the

weak van der Waals force between the matrix and the reinforcement.⁸ In order to develop nanocomposite materials with excellent mechanical properties, strong chemical bonding between the reinforcement and the matrix is a necessary, but not sufficient, condition.

In a previous experimental investigation,¹¹ we employed graphitic carbon nanofibers (GCNFs) as reinforcements in polymeric matrix nanocomposites. Strong and stiff GCNFs (Young's modulus $E > 600$ GPa) have average diameters as small as 25 nm and demonstrate atomic structures such that edge carbon atom surface sites are present along the entire length of the carbon nanofiber. Chemical modification of these surface carbon sites and subsequent reaction with bifunctional linker molecules provides surface-derivatized GCNFs that can covalently bind to polymer resin molecules. This nanofiber/polymer covalent binding is expected to delay interfacial debonding. So far, it has been difficult to quantify the improved interfacial bonding between the matrix and the nanofibers accurately

*Author to whom correspondence should be addressed.

(i.e., by direct measurement at the nanoscale). However, mechanical properties of the final macroscale nanocomposite materials can be easily measured with various kinds of standard tests for engineering materials. To achieve maximum utilization of the properties of nanofibers, uniform dispersion and good wetting of the nanofibers within the matrix must be ensured.¹² All these local interfacial properties affect the macrolevel material behavior. For example, it was reported that there was as much as a 10% decrease in flexural strength in nanotube/epoxy composite beams due to weakly bonded interfaces.¹³ Also, significant reduction in composite stiffness was attributed to local nanofibers/nanotube waviness.^{14,15} Our macroscale mechanical property characterizations including bending, tensile, and fracture properties showed that there was very little increase in mechanical properties of nanocomposites, although we used reactive linkers to improve the fiber/matrix interface.¹¹

We suspect that the local interfacial stress level in nanocomposites would be much higher than that in traditional composites because of high property mismatch between the nanoscale reinforcement and the matrix. Since high interfacial stress may lead to interfacial debonding and then final failure of nanocomposites, this may contribute to the low failure strains in nanocomposites observed in many recent experiments.^{11,12} Also, the advantage of small diameters of nanofibers or nanotubes is an increased interfacial contact area with the matrix, while its shortcoming is a high possibility of initial interfacial defects, which may lead to low failure strain of nanocomposites. Therefore, a theoretical analysis of interfacial stress transfer and stiffness and strength mismatch between the nanoscale reinforcement and the matrix will be much needed before we design and produce extensive varieties of nanocomposite materials. As illustrated in Figure 1, both the final failure strain (3.3%) and Young's modulus (2.9 GPa) of the pure epoxy are low. However, both the final failure strain (up to 10.0%) and Young's modulus (up to 1000 GPa) of the nanotube or nanofibers are extremely high, so the properties of the nanoscale reinforcement and the matrix are highly

mismatched. A key question of nanocomposite design is if these two types of materials are mixed (even if strong interfacial bonding was ensured), would the final composite properties (here we refer to the mechanical properties of discontinuous nanofiber/nanotube composites) show a reasonable increase over those of the matrix? Generally, it has been found that the stiffness properties of nanocomposites are always higher than those of the pure matrix. However, the final strength of the nanocomposite may or may not exceed the strength of the pure matrix if discontinuous nanofibers/nanotubes (even if they were aligned) are used in nanocomposites. As seen in Figure 1, the stress–strain curve of the nanocomposites is always steeper than that of the pure matrix if we employ linear elasticity theory to simplify the explanation. Therefore, the final strength of the nanocomposites is mainly determined by the final failure strain of the nanocomposites. Unfortunately, the latter value was always lower than that of the pure matrix and significantly decreased with the increase of nanofiber/nanotube weight/volume percents as ascertained by numerous experimental studies.

2. FINITE ELEMENT MODELING

The main purpose of this investigation is to seek the mechanical reasons of low failure strains of the nanocomposites. Our major task is to examine the interfacial stress transfer, which is critical due to high property mismatch of the nanoscale reinforcement and the matrix. Finite element analysis (FEA) was chosen as the primary tool for analysis instead of molecular dynamics simulations, since the latter could only deal with physical phenomena at the level of a few nanometers at the current stage, while the size of a representative volume of a nanocomposite material ranges from 10 nm upward to several hundreds of nanometers.¹⁶ Since the smallest dimension of our nanofiber lies in the range 20–50 nm, continuum mechanics assumptions, such as those used in finite element analysis, are still valid at such length scales. Similar finite element analyses have been reported by Fisher et al.¹⁴ and Chen and Liu¹⁶ with a focus on stiffness analysis incorporating micromechanics theory. It is noted that these finite element analyses simplified the complex interaction among the nanoscale reinforcement, matrix, and the possible interphase. The interphase issue has received considerable attention in nanocomposite systems, since nanoscale reinforcement affords a greater interphase volume compared to traditional composite materials. However, it is very difficult to determine the physical properties, such as thickness, of the interphase and they may certainly not be treated as material constants. From this viewpoint, the concept of interphase and its modeling is not employed in this investigation.

In this investigation, our objective is to investigate and reduce the interfacial stresses. Two separate cases are (a) baseline nanocomposites subjected to tension and shear

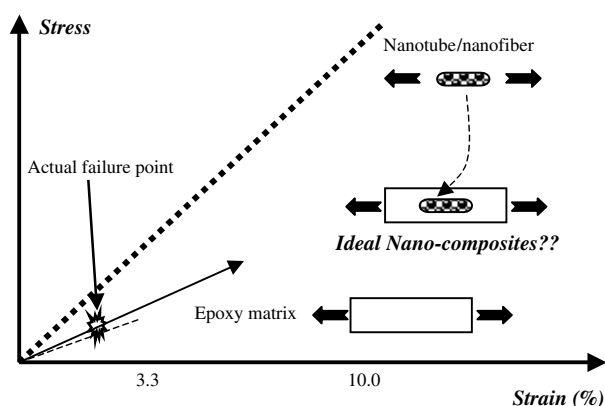


Fig. 1. Nanocomposite design based on stress–strain curves.

loading and (b) nanocomposite systems with modified nanofiber ends. Similar end modifications were effectively used to remove the interfacial stress singularity in macroscale dissimilar material joints through an integrated numerical and experimental investigation by Xu et al.¹⁷ Since direct nanoscale experimental validation is very difficult to conduct at the current stage, we mainly focus on numerical investigation. Although the nanofiber-reinforced composite is the main focus, the numerical analysis can be easily extended to nanotube-reinforced composite by varying the stiffness and dimensions of the nanoscale reinforcement.

Figure 2a is a transmission electron microscopy (TEM) image showing short nanofibers well-dispersed in an epoxy matrix. Usually, these nanofibers are curved and therefore the improvement in composite stiffness is not high.¹⁴ Based on the material analysis, a basic representative volume element for mechanics analysis (henceforth referred to as RVE) is shown with typical dimensions and boundary conditions in Figure 2b. Figure 2c shows the full RVE for shear loading case, with different boundary conditions. The volume fraction of the nanofiber/nanotube in the baseline RVE was 4%, and this percentage was

increased to 11% by retaining the dimensions of the nanofiber and decreasing the dimensions of the epoxy matrix. A commercial FEA software ANSYS was used for numerical analysis. A transition mesh, using PLANE42 elements, was employed for the elements to fan out from a dense mesh in and around the nanofiber–epoxy matrix interface to a relatively coarser mesh utilized for the rest of the RVE. The material properties used in the baseline RVE were epoxy matrix, $E_m = 2.6$ GPa, $\nu_m = 0.3$, and nanofibers, $E_f = 600$ GPa, $\nu_f = 0.3$. Similar to other finite element analyses, these nanofibers were treated as transversely isotropic materials.^{14,16} The elastic modulus of the nanofiber was varied such that four typical reinforcement cases were considered: $E_f = 50$ GPa (glass fibers), 200 GPa (carbon fibers), 600 GPa (graphite nanofibers), and 1000 GPa (carbon nanotubes). Remote tensile stress of 10 MPa ($= 0.01$ nN/nm²) was applied along the shorter edge of the epoxy matrix and a linear, elastic analysis was run to determine the dependence of interfacial stresses on elastic properties and volume fractions. The analyses were varied in terms of (a) applied stress of 10 MPa or (b) applied displacement of 0.1 nm to the RVE.

If two dissimilar materials are joined, interfacial stress components may be singular—hence a special approach will be employed to characterize their distributions:¹⁸

$$\sigma_{ij}(r, \theta) = \frac{K}{(r/L)^\lambda} f_{ij}(\theta) + \sigma_{ij0}(\theta) \quad (1)$$

Here r and θ are polar coordinates, L is a characteristic length, K is the stress intensity factor, and the constant stress term σ_{ij0} has been defined such that for mechanical loading perpendicular to the interface, $\sigma_0 = 0$. Also, $f_\theta(\theta)$ was defined in such a way that $f_\theta(\theta = 0) = 1$. Taking the logarithm of both sides of Eq. 1, the stress intensity factor K can be obtained from the numerical interfacial stress distribution of $\log(\sigma_\theta^{FE}(r, \theta) - \sigma_{\theta0}(\theta))|_{\theta=0}$ versus $\log(r/L)$. In this investigation, the radius of the nanofiber r_f is taken as the characteristic length L . The calculation of the stress singularity order λ was based on the determinant $f(\theta_1, \theta_2, \alpha, \beta, p)$ introduced in Ref 19. For any particular material combination, the Dundurs' parameters α and β were calculated, which represent stiffness mismatch of two joint materials.²⁰ Besides, the joining angles for two kinds of materials were known: 90° for the nanofiber and 270° for the epoxy matrix. As such, the only unknown parameter $p (= 1 - \lambda)$ could be determined from the equation

$$D(a, b, \alpha, \beta, p) = A\beta^2 + 2B\alpha\beta + C\alpha^2 + 2D\beta + 2E\alpha + F = 0 \quad (2)$$

Where the coefficients A, B, C, D, E , and F depend on the joining angles and λ .

3. RESULTS AND DISCUSSION

Owing to different loadings applied to the RVE, very different interfacial stress distributions along the short interface between the matrix and the nanofiber with straight

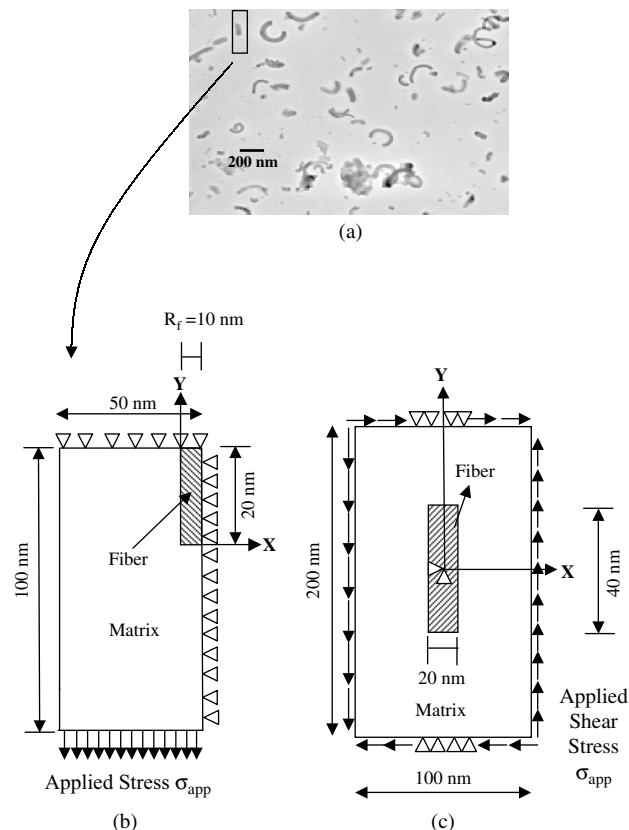


Fig. 2. (a) Transmission electron microscopy (TEM) image of nanofibers as dispersed in GCNF/epoxy nanocomposite and (b) representative volume element (RVE) used for micromechanical analysis of nanofiber-epoxy nanocomposite under tension, $\sigma_{app} = 0.01$ nN/nm², $V_f = 4\%$. A quarter of the original RVE is shown here with symmetric boundary conditions. (c) same RVE under shear loading.

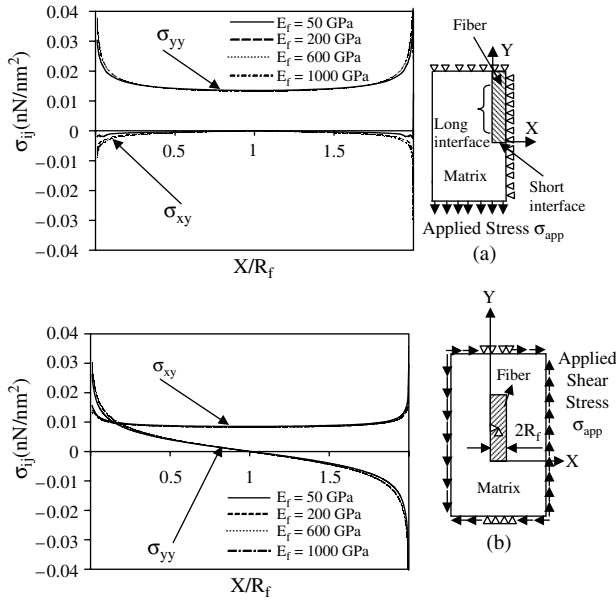


Fig. 3. Effect of applied loading types on the interfacial stress distributions (a) along the short interface for tension loading and (b) along the short interface for shear loading (full specimen analyzed). $V_f = 4\%$. Applied stress = 10 MPa.

ends were obtained, as illustrated in Figure 3a,b. While the interfacial normal stress in the tensile loading case remains positive in nature along the length of the short interface, Figure 3b shows that the interfacial normal stress along the short interface changes from a positive value (tensile) to a negative value (compressive). This means that under shear loading, one end of the fiber is “pulled down” while the other end is “pushed out.” Therefore, we may expect that the same nanofiber-reinforced composite would yield higher ultimate strengths or strains under shear loading as compared to tensile loading. It was also noticed that a higher Young’s modulus of the reinforcement led to higher interfacial stresses for both loading cases. However, severe stress singularity at the finite end of the nanofiber existed for both cases and would surely induce a macroscale crack to cause final composite failure.

Figure 4 depicts the variation of the stress singularity order with Young’s moduli mismatch between the matrix

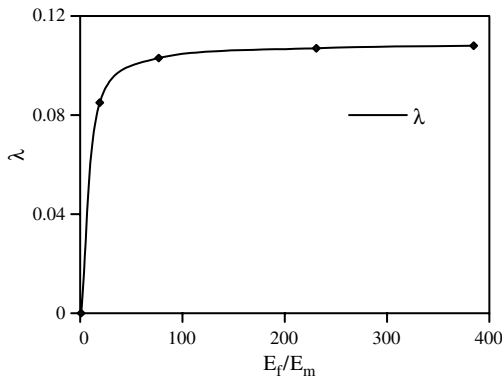


Fig. 4. Effect of Young’s moduli mismatch on stress singularity order.

and the nanofiber. Since the singular stress values prevent accurate comparisons for different material combinations, the stress singularity orders were computed to compare different E_f/E_m cases. The starting point of the stress singularity order curve corresponds to the case where there is no property mismatch or zero stress singularity order. This curve shows a smooth transition and reaches a plateau gradually as E_f/E_m assumes a larger value.

Figure 5 depicts the effect of volume fraction on the interfacial shear and normal stress distributions along the short and long interfaces, in response to applied stress of 10 MPa. While an increase in volume fraction showed little effect on the stress distributions along the short interface, the interfacial shear stress along the long interface seems to be least for the baseline volume fraction $V_f = 4\%$ and increases slightly with increasing volume fraction. This would mean that a high volume/weight fraction of nanofibers has little influence on the local interfacial stress state or on the final failure strain of the nanocomposite material. However, this was contradicted in the applied tensile strain case. Figure 6 depicts the effect of the nanofiber volume fraction on the interfacial shear and normal stresses along the short and long interfaces, in response to applied displacement of 0.1 nm (tensile strain case). An increase in volume fraction

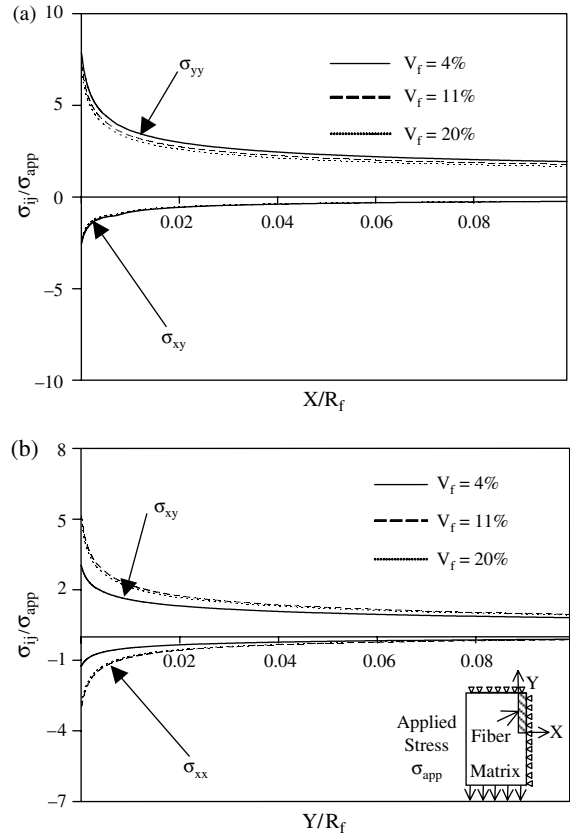


Fig. 5. Effect of nanofiber volume/weight percents on interfacial stress. (a) Short interface under applied stress of 10 MPa and (b) long interface under the same applied stress.

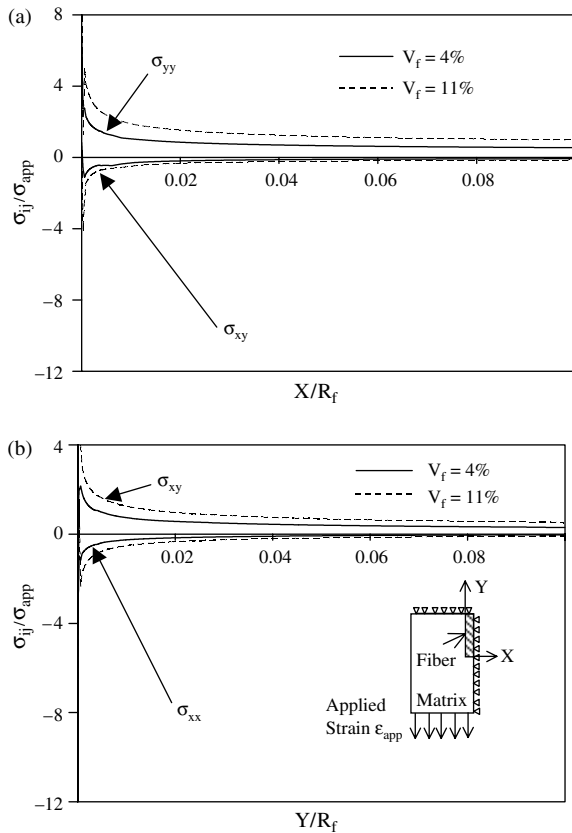


Fig. 6. Effects of the nanofiber volume percents on the interfacial stress distributions (a) along the short interface under applied displacement 0.1 nm and (b) along the long interface under the same applied displacement.

showed a corresponding increase of the interfacial stress distributions. These results provide mechanic insight for recent experimental results:^{11, 12} high volume/weight fractions of nanoscale reinforcements lead to lower ultimate failure strains of nanocomposite materials.

The possible singular interfacial stresses at the rectangular nanofiber ends are not the only reasons for low failure strengths or strains—another important issue is interfacial stress transfer. Figure 7 shows the effect of geometry of the nanofiber end on the interfacial stress distributions. Two cases were considered: (a) the baseline case with straight edge forming a 90° angle at the interface corner and (b) a round interface corner with a radius of 1 nm. As expected, the normal stress over the short interface showed a strong singularity in case (a) but not so in case (b). Shear stress variation along the long interface depicted in Figure 7b also shows a significant reduction around the interfacial corners. Hence, nanofibers with slightly rounded edges are a better alternative to common nanofibers with straight edges. Similar conclusions for traditional fiber-reinforced composites were drawn by Sun and Wu²¹ and Liou.²² However, the normal stress distribution of the nanofiber did not change significantly by shaping the nanofibers. Besides, from the composite

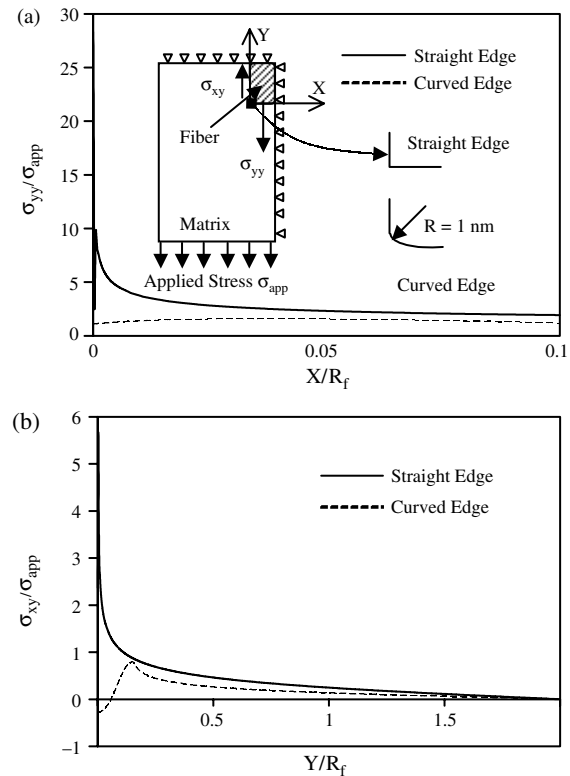


Fig. 7. Effect of the nanofiber end on the interfacial stress distribution (a) normal stress variation along short interface and (b) shear stress variation along the long interface for $V_f = 4\%$, $E_f = 600$ GPa, and applied stress = 10 MPa.

processing viewpoint, rounded ends for each nanofiber would prove to be very time-consuming and costly.

The effects of both volume fractions and Young’s moduli on the normal stress distribution along the midplane of the nanofibers with straight or curved edges have also been examined in Figure 8a,b. The normalized stress is seen to rise toward the center of the fiber as a result of interfacial shear transfer, or shear-lag effect.^{23, 24} However, the maximum normal stress in the nanofiber is only around 1.6 times that in the matrix, far below the strength ratio of the nanofiber/nanotubes over the polymeric matrix (at least 100). Although some research results showed that modified ends/edges of the short fibers could effectively remove the stress concentration/singularity,^{21–23} the normal stress distribution of the short fiber is not altered significantly. Therefore, such composite design will not make full use of the high strength of nanofibers/nanotubes. Discontinuous nanotubes/nanofibers with high strength and stiffness, when added as reinforcement to matrices, are undermined by the stress singularity at the fiber–matrix interface and also by the inefficient interfacial shear stress transfer even if nanofiber ends were rounded by means of special processing. This provides us with an important principle for nanocomposite design.

It should be noted that the finite end stress singularity is a theoretically elastic phenomenon and will never occur

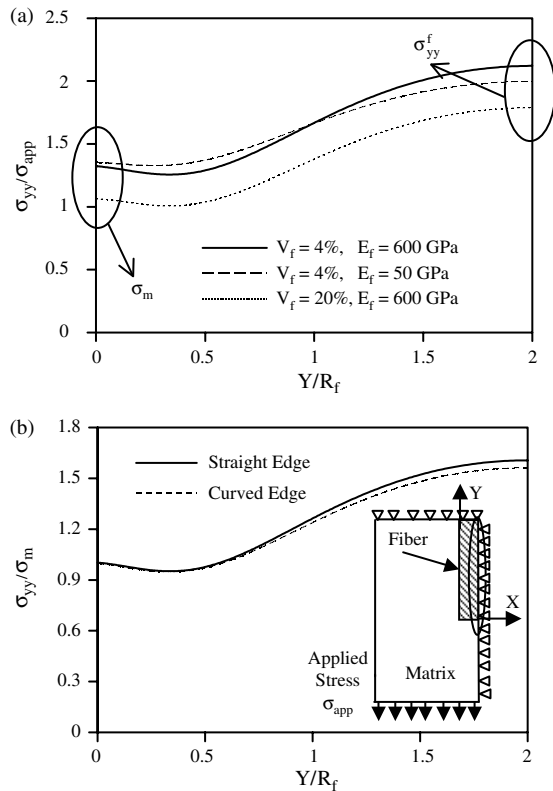


Fig. 8. Nanofiber stress distribution under tensile load (midfiber stress). (a) Variation with Young's modulus and volume fraction and (b) for straight-edged and round-edged nanofiber. Radius of round-edged nanofiber = 1 nm. σ_m = normal stress inside the matrix; σ_{yy}^f = normal stress inside the fiber. $V_f = 4\%$, $E_f = 600$ GPa, applied stress = 10 MPa.

in reality. A significant reduction in singularity has been noticed when more accurate models are used to depict the polymeric matrix (e.g., elastoplastic, viscoelastic model) in traditional composites with graphite fibers. In addition, for nanotube-reinforced composites, since the nanotube has a lattice-type structure at the nanometer level, the actual singularities that occur at the interface should be much lower than those predicted by using the continuum mechanics approach. Therefore, these two arguments lead to the conclusion that the singularities predicted in this investigation are overestimated. However, the interfacial shear stress concentration (due to the theoretical stress singularity) definitely becomes more severe if the stiffness mismatch of the reinforcement and the matrix increases, which in turn will lead to interfacial debonding.

4. CONCLUSIONS

Discontinuous nanotubes/nanofibers with high strength and stiffness, when added as reinforcement to matrices, are undermined by the stress singularity at the fiber–matrix interface and also by inefficient interfacial shear

stress transfer. However, continuous forms of nanofibers or nanotubes without finite ends, on the other hand, preclude the presence of extra matrix material at the ends of fibers and hence eliminate stress concentration/singularity. Thus, for future nanocomposite material designed with an objective of strength or fracture toughness increase,^{11,25} discontinuous nanofibers or nanotubes (in spite of being aligned) are not recommended.

Acknowledgments: L. R. X. gratefully acknowledges the support from the Office of Naval Research Young Investigator Award (N00014-03-1-0505, Dr. Roshdy G. S. Barsoum, Program Officer) and the National Science Foundation, Surface Engineering and Materials Design Program (CMS-0409665, Dr. Yip-Wah Chung, Program Director).

References and Notes

1. M. M. J. Treacy, T. W. Ebbesen, and T. M. Gibson, *Nature* 381, 678 (1996).
2. K. T. Lau and D. Hui, *Comp. Part B* 33, 263 (2002).
3. D. Qian, G. J. Wagner, W. K. Liu, Y. Min-Feng, and R. S. Ruoff, *Appl. Mech. Rev.* 55, 495 (2002).
4. J. J. Luo and I. M. Daniel, *Comp. Sci. Technol.* 63, 1607 (2003).
5. H. D. Wagner, O. Lourie, Y. Feldman, and R. Tenne, *Appl. Phys. Lett.* 72, 188 (1998).
6. D. Qian, E. C. Dickey, R. Andrews, and T. Rantell, *Appl. Phys. Lett.* 76, 2868 (2000).
7. M. F. Yu, O. Lourie, M. Dyer, K. Moloni, T. Kelly, and R. S. Ruoff, *Science* 287, 637 (2000).
8. L. S. Schadler, S. C. Giannaris, and P. M. Ajayan, *Appl. Phys. Lett.* 73, 3842 (1998).
9. G. M. Odegard, T. S. Gates, K. E. Wise, C. Park, and E. J. Siochi, *Comp. Sci. Technol.* 63, 1671 (2003).
10. E. T. Thostenson, Z. Ren, and C.-W. Chou, *Comp. Sci. Technol.* 61, 1899 (2001).
11. L. R. Xu, V. Bhamidipati, W. H. Zhong, J. Li, C. M. Lukehart, E. Lara-Curzio, K. C. Liu, and M. J. Lance, *J. Comp. Mater.* 38, 1563 (2004).
12. W. H. Zhong, J. Li, L. R. Xu, J. A. Michel, L. M. Sullivan, and C. M. Lukehart, *J. Nanosci. Nanotechnol.*, in press.
13. K. T. Lau, S. Q. Shi, L. M. Zhou, and H. M. Cheng, *J. Comp. Mater.* 37, 365 (2003).
14. F. T. Fisher, R. D. Bradshaw, and L. C. Brinson, *Comp. Sci. Technol.* 63, 1689 (2003).
15. D. Srivastava, C. Wei, and K. Cho, *ASME Appl. Mech. Rev.* 56, 215 (2003).
16. X. L. Chen and Y. J. Liu, *Comp. Mater. Sci.* 29, 1 (2004).
17. L. R. Xu, H. Kuai, and S. Sengupta, *Exp. Mech.*, in press.
18. D. Munz and Y. Y. Yang, *Int. J. Fract.* 60, 169 (1993).
19. D. B. Bogy, *J. Appl. Mech.* 38, 377 (1971).
20. J. W. Hutchinson and Z. Suo, *Adv. Appl. Mech.* 29, 63 (1992).
21. C. T. Sun and J. K. Wu, *J. Reinf. Plast. Comp.* 3, 130 (1983).
22. W. J. Liou, *Compu. Struct.* 62, 999 (1997).
23. R. F. Gibson, *Principles of Composite Material Mechanics*, McGraw-Hill Inc., New York (1994).
24. W. J. Baxter, *J. Mater. Sci.* 33, 5703 (1998).
25. S. Roy, H. Lu, S. Periasamy, and J. Ma, in *Proceedings of the 44th AIAA/ASME/ASCE/AHS Structures, Structural Dynamics, and Materials Conference*, Norfolk, VA (2003).